INTERFACE SCIENCE 9, 35–42, 2001

Evaluating Anisotropic Surface Energies Using the Capillarity Vector Reconstruction Method

DAVID M. SAYLOR AND GREGORY S. ROHRER*
Department of Materials Science and Engineering, Carnegie Mellon University, Pittsburgh, Pennsylvania 15213-3890, USA
grzo@andrew.cmu.edu

Abstract. By measuring the geometry and crystallography of the three interfaces that meet at grain boundary thermal grooves, it is possible to determine the anisotropy of the surface free energy. Previously, the surface energy of MgO at 1400°C in air was approximated by a truncated double Fourier series with coefficients that were determined by fitting the observations to Herring's condition for local equilibrium at a triple junction. The purpose of this paper is to describe an alternative analysis of the same data set that is not limited by an assumed functional form of the surface energy. In this case, the space of surface characters is discretized and each orientation is associated with a capillarity vector (according to the Cahn–Hoffmann definition). The set of capillarity vectors that most closely satisfies the condition for local equilibrium at each triple junction is then determined by an iterative method. The relative surface free energies derived from this analysis are more anisotropic than those derived from the series fit and more consistent with the observed faceting of MgO in air at 1400°C. The relative surface energies of the low index planes are $\gamma_{110}/\gamma_{100} = 1.07 \pm 0.04$ and $\gamma_{111}/\gamma_{100} = 1.17 \pm 0.04$.

Keywords: surface energy, magnesia, grain boundary grooves, atomic force microscopy, capillarity vector

Introduction

In a previous paper [1], geometric and crystallographic observations at grain boundary thermal grooves were used to experimentally evaluate the anisotropy of the surface energy of magnesia after annealing at 1400°C in air. The method employed in that paper was adapted from previous studies of metallic systems, where the surface energy was approximated by a truncated double Fourier series [2, 3]. The unknown coefficients of the series were determined by fitting the observations to Herring's [4] condition for local equilibrium at the triple junction. Throughout this paper, we will refer to this procedure as the series fitting method. One limitation of the series fitting method is that the assumption of particular basis functions for the finite series constrains the form of the resulting surface energy function. The comparative advantages and disadvantages of different basis functions were described by Gale et al. [5] who evaluated the orientation dependence of the surface energy of an Fe-3% Si alloy. This work showed that while a conventional trigonometric series can produce cusps in the surface energy function, it does not have the correct symmetry. Spherical harmonic basis functions can be used to produce a surface energy with the correct symmetry, but the finite extent of the series makes it impossible to produce sharp cusps at low energy orientations. The objective of the present paper is to describe an alternative method for reconstructing the surface energy anisotropy from thermal groove measurements that does not parameterize the surface energy in terms of a harmonic series. Here, we employ a procedure developed by Morawiec [6] that provides discrete values of the surface energy for a predefined set of surface normals. This discrete analysis is facilitated by use of the Cahn–Hoffman [7, 8] formalism for the capillarity vector which makes it possible to include the surface torques in the equilibrium equation

*To whom all correspondence should be addressed.

without having to compute differentials. This method will be referred to as the capillarity vector reconstruction method.

The condition for local equilibrium at a triple junction with anisotropic interfacial energies that relates the interfacial geometry and crystallography to the energies of the three interfaces was originally described by Herring [4]:

$$\sum_i \gamma_i \hat{t}_i + \frac{\partial \gamma_i}{\partial \beta_i} \hat{n}_i = 0. \tag{1}$$

In Eq. (1), γ_i is the excess free energy per unit area of the ith interface, $\hat{t}_i$ is the unit vector that lies in the ith interface and points in a direction perpendicular to and away from the line of intersection of the three interfaces ($\hat{l}$), $\hat{n}_i$ is the unit vector normal to the line of intersection such that $\hat{n}_i = \hat{l} \times \hat{t}_i$, and β_i is the right handed angle of rotation about $\hat{l}$ for the ith boundary measured from a reference direction. By approximating the orientation dependence of the surface energy as a finite series, γ_i and $\partial\gamma_i/\partial\beta_i$ can be computed directly from the best fit function.

The equilibrium condition in Eq. (1) can be rewritten in terms of the Cahn–Hoffman [7, 8] capillarity vector, $\vec{\xi}$, as illustrated in the following paragraphs. The capillarity vector is formed by combining the two scalar quantities γ_i and $\partial\gamma_i/\partial\beta_i$ with unit vectors normal and parallel to the plane of the interface, respectively. The component of the capillarity vector normal to the interface is equal in magnitude to γ, thus $\vec{\xi}_n = \gamma\hat{n}$. Note that $\vec{\xi}_n \times \hat{l}$ is a tension in the plane of the interface that is perpendicular to $\hat{l}$ and has a magnitude of γ:

$$\vec{\xi}_n \times \hat{l} = \gamma\ \hat{t}. \tag{2}$$

Furthermore, the capillarity vector has a component in the plane tangent to the interface that is related to the change in γ with orientation given by $\vec{\xi}_t = (\partial\gamma/\partial\beta)_{\max}\hat{t}_0$, where $\hat{t}_0$ points in the direction of maximum increase of γ. Therefore, $\vec{\xi}_t \times \hat{l}$ is a vector perpendicular to the interface whose magnitude is given by the component of $\vec{\xi}_t$ perpendicular to $\hat{l}$. This is a measure of the so-called torque force that is normal to the interface and urges it to rotate about the line of intersection. In other words,

$$\vec{\xi}_t \times \hat{l} = \frac{\partial\gamma}{\partial\beta}\hat{n}. \tag{3}$$

Substituting the left hand sides of Eqs. (2) and (3) into Eq. (1), we see that Herring's [4] equilibrium condition for a triple junction can be expressed in the following way:

$$(\vec{\xi}^{\,1} + \vec{\xi}^{\,2} + \vec{\xi}^{\,3}) \times \hat{l} = 0, \tag{4}$$

where the indices 1, 2, and 3 correspond to surface 1, surface 2, and the grain boundary depicted in Fig. 1. By fitting experimental observations to Eq. (4), the capillarity vectors for the interfaces bounding a thermal groove can be determined without evaluating any differential terms. The surface energy is then given by the magnitude of the capillarity vector normal to the surface plane.

In the present paper, we compare the performance of the series fitting method with that of the capillarity vector reconstruction method on a simulated and real data set. The two methods produce results that are qualitatively similar. However, there are significant quantitative differences. In the case of the simulated data, the surface energy derived from the capillarity vector reconstruction method reproduces the input surface energy more accurately than the series fitting method. One of the principal limitations of the series fitting method is that it underestimates the total anisotropy. This trend is apparently reproduced in the real data, as the surface energy that results from the capillarity vector reconstruction method is more anisotropic than the surface energy that results from the series fitting method. Because the results from the capillarity vector reconstruction method are more consistent with experimentally observed surface faceting, we conclude that this method of determining the surface energy anisotropy is superior to the series fitting method.

Methods

(i) Experimental

The details of the methods used for both the experimental observations and the series fitting method have been described in a previous paper [1]. Breifly, the technique involves measuring the geometry and crystallography of thermal grooves around the circumference of a few fully or partially enclosed grains in a typical polycrystal, a situation depicted in Fig. 1(a). The orientations of both the enclosed and matrix grains are determined by backscattered electron diffraction. Atomic force microscopy is used to determine the surface inclinations (χ_i) and the angle between $\hat{e}_1$ and $\hat{v}$, as defined in Fig. 1(a). Serial sectioning is used to determine the

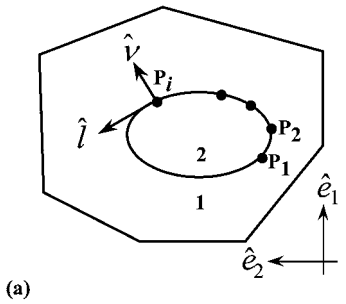

(a)

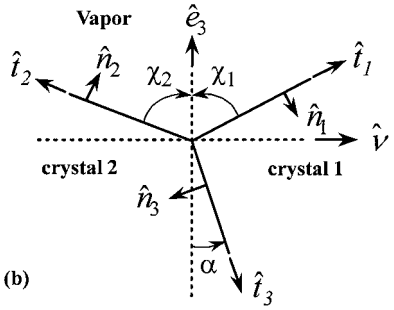

(b)

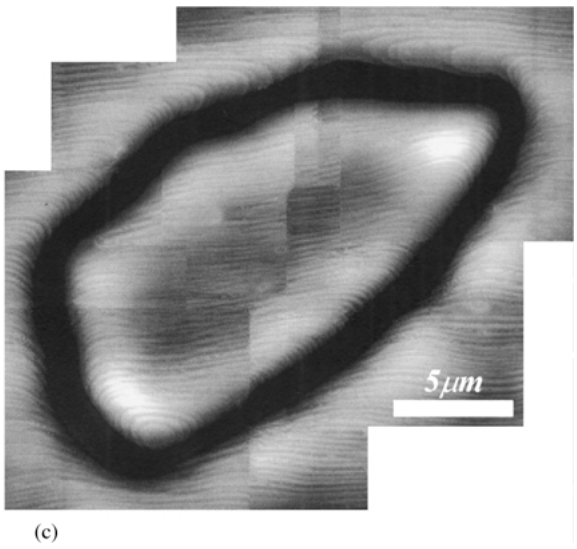

(c)

Figure 1. The coordinate system used for the data analysis. (a) A schematic plane view of an enclosed grain (labeled 2) within a matrix grain (labeled 1). Multiple groove measurements are made around the circumference of the enclosed grain, at points labeled P_i. (b) A schematic cross-sectional view of a triple junction. Note that $\hat{l}$ points into the plane of the paper. (c) AFM image montage depicting an enclosed grain. The enclosed grain is misoriented from the surrounding grain by 3.6°. The black to white contrast in the image is approximately 150 nm.

grain boundary inclination, α. These data allow the surface energy to be reconstructed using either the series fitting technique or the capillarity vector reconstruction method. The final data set consisted of parameters from 269 thermal grooves measured around the circumference of five enclosed grains in a polycrystalline magnesia sample which had been annealed in air for 5 h at 1400°C.

(ii) The Capillarity Vector Reconstruction Method

The capillarity vector reconstruction method involves finding a consistent set vectors, $\vec{\xi}_i$, that satisfy Eq. (4) as nearly as possible for all of the observed thermal grooves. While we wish to know the capillarity vectors with respect to the crystal coordinate system, Eq. (4) holds only for vectors in the sample coordinate system. The orthogonal matrix, g_{jl}, that transforms a vector from the sample reference frame to the crystal reference frame is [9]:

$$g(\phi_1,\ \Phi,\ \phi_2) = \begin{bmatrix} c\phi_1 c\phi_2 - s\phi_1 s\phi_2 c\Phi & s\phi_1 c\phi_2 + c\phi_1 s\phi_2 c\Phi & s\phi_2 s\Phi \\ -c\phi_1 c\phi_2 - s\phi_1 s\phi_2 c\Phi & -s\phi_1 s\phi_2 + c\phi_1 c\phi_2 c\Phi & c\phi_2 s\Phi \\ s\phi_1 s\Phi & -c\phi_1 s\Phi & c\Phi \end{bmatrix}, \tag{5}$$

where ϕ_1, Φ, and ϕ_2 are the Eulerian angles and the symbols s and c represent sine and cosine, respectively. We can therefore rewrite Eq. (4) as:

$$\varepsilon_{ijk}\, l_k g^{s}_{lj} \xi^{s}_{l} = 0, \tag{6}$$

where ε_{ijk} is permutation tensor and the enumeration of the superscript s goes from 1 to 3 to represent surface 1, surface 2, and the grain boundary, respectively. For s equal to 1 or 2, the Eulerian angles in Eq. (5) are those describing the orientation of the appropriate crystallite with respect to the sample reference frame. Since we do not sample enough of the possible grain boundary characters, we are forced to assume that the grain boundary torque is negligible. In other words, $\partial\gamma_3/\partial\beta_3 = 0$ in Eq. (1) and $\vec{\xi}^{\,3}$ must be perpendicular to the grain boundary plane. To apply this constraint, only the first component of $\vec{\xi}$ is considered (if $s = 3, l = 1$). Therefore, the Eulerian angles, ϕ_1, Φ, and ϕ_2, that specify the grain boundary ($s = 3$) orientation are θ, $3/2\pi$, and $\pi - \alpha$, respectively.

Because we seek a discrete set of capillarity vectors, the space of interface characters must be discretized over a fixed domain. One can chose the entire domain

of possible surface orientations, the fundamental zone of indistinguishable orientations, or an appropriate sub-domain containing a integer number of fundamental zones. We used a convenient sub-domain that contains all directions specified by surface unit normals that have all three perpendicular components greater than or equal to zero. If we specify these directions using the spherical coordinates, these are the values of θ and ϕ between 0 and 90°. This domain is then discretized in units of $\Delta \cos\theta$ and $\Delta\phi$, which makes the range of surface normals in each cell the same. Because we are assuming $\partial\gamma_3/\partial\beta_3 = 0$, each enclosed grain boundary has only one character specified by the misorientation. Thus, the space of grain boundaries is discretized simply by the enclosed grain from which the measurement was taken. In both cases, the discrete cells are enumerated with an index, β. For all surface normals that fall within a given cell, the capillarity vector is approximated by the value of $\vec{\xi}$ assigned to that cell.

For each of the J observed triple junctions, there are three equilibrium equations enumerated by i, representing the force balance in the three perpendicular directions. To solve these equations, we make the substitution that for an orientation in cell β, $A^{\beta}_{il} = W\varepsilon_{ijk}\, l_k g_{lj}$, where W is selected so that $A^{\beta}_{il}A^{\beta}_{il} = 1$, with no summation over i. The set of J linear equations representing the balance of interfacial forces is now:

$$A^{\beta}_{Jil}\xi^{\beta}_{l} = 0. \tag{7}$$

The system of equations is solved using the iterative method described in Ref. [6]. The process begins with the assumption that $\xi^{\beta}_{l} = \hat{n}^{\beta}_{l}$ where $\hat{n}^{\beta}_{l}$ is the unit normal vector at the center of each cell. At each step, the deviation vector, Δ_{Ji}, in the sample coordinate system is calculated according to:

$$A^{\beta}_{Jil}\xi^{\beta}_{l} = \Delta_{Ji}. \tag{8}$$

Because our sub-domain of surface character space contains six symmetrically indistinguishable cells for each possible normal vector, there are 36 equivalent equations for each observed triple junction. Therefore, the deviation vector for each triple junction is actually the average of the 36 symmetrically equivalent equations. After Δ_{Ji} is calculated for each thermal groove, the capillarity vector is modified by the product of the deviation vector (in the crystal coordinate system) and a relaxation factor, ω. On the kth iteration, it is modified in the following way:

$$\xi^{\beta}_{[k]} = \xi^{\beta}_{l[k-1]} - \omega A^{\beta}_{Jil}\Delta_{Ji[k-1]}. \tag{9}$$

The relaxation factor is chosen as the inverse of the maximum number of equations that any one interfacial character is involved in. At the end of each iteration, the $\vec{\xi}$ values are normalized by dividing them by the average magnitude of all $\vec{\xi}$ at the current iteration step. The iteration process is stopped when the change in the sum of the magnitude of all of the deviations vectors is less than 1% of the change during the first iteration.

Because the data collection technique does not generate a uniform distribution of surface characters, the cell population is nonuniform and many of the cells are underpopulated. This can create sharp variations in what we expect to be a continuous and relatively smooth field of capillarity vectors. For this reason, the field of capillarity vectors is smoothed after the last iteration. The value of $\vec{\xi}$ in each cell is replaced by an average of that cell and the eight adjacent cells in the unsmoothed matrix. Cells at the edges and corners of the matrix are averaged only with their existing neighbors, and if a cell contains zero or one observation, the cell is not used in the smoothing process. Tests on model data sets suggest that with a denser distribution of data, the smoothing process is not required.

After smoothing the field of $\vec{\xi}$, the energy (γ) for each orientation, $\hat{n}$, is determined by $\gamma = \vec{\xi}\cdot\hat{n}$. The energy of each surface is taken to be the average of the energies in all symmetrically equivalent cells.

Results

(i) Testing on Simulated Data

To test the reconstruction method, we generated a set of data based on a model energy function. The model function was isotropic ($\gamma_s = 1$) everywhere except for a cusp around (111). The cusp had a width of 15° and a depth of $0.6\gamma_{\text{isotropic}}$ and was shaped by an analogy to the Read–Shockley expression for the energy of low angle grain boundaries. The functional form is given by:

$$\begin{aligned} \gamma(0) &= 0.6 \\ \gamma(\theta_{111}) &= 0.4\left(\frac{\theta_{111}}{15}\right)\left(1 - \ln\left(\frac{\theta_{111}}{15}\right)\right) + 0.6 \qquad 0 < \theta_{111} \le 15^{\circ} \\ \gamma(\theta_{111}) &= 1 \qquad\qquad \theta_{111} > 15^{\circ} \end{aligned} \tag{10}$$

where θ_{111} is the angular separation, in degrees, between the surface orientation and [111].

The model thermal grooves were generated by first assigning Euler angles (ϕ_1, Φ, ϕ_2) to both the enclosed and matrix grains. Values for χ_i and $\hat{\nu}$ were then randomly generated. Next, the values of χ_2 and α that balance the interfacial energies according to Eq. (1) were determined using a downhill simplex method [10]. Parameter sets for simulated grooves were considered valid if the absolute values of the components of Eq. (1) that are perpendicular and parallel to the macroscopic sample surface summed to less than 0.01. The procedure was repeated until 50 valid grooves were found for each of five enclosed grain/matrix grain pairs. In other words, the number of observations in the model data set was selected to mimic as nearly as possible the real data set. Since the real data contains experimental errors, the groove parameters (χ_1, χ_2, $\hat{\nu}$, and α) were perturbed by a random angle generated according to a Gaussian distribution with standard deviations of 1°, 1°, 1°, and 5°, respectively.

The model energy function is shown in Fig. 2 together with a comparison of the results from the series fitting method and the capillarity vector reconstruction. The fitting for the series reconstruction method was conducted exactly as previously described, using an R = 1 series [1]. The Fourier series fit results in a smoothly varying function that approximates the shape of the actual surface energy function. However, the true depth of the cusp is underestimated. For the capillarity vector reconstruction method, the sub-domain of surface characters was divided into 15 equal sections in $\cos(\theta)$ and ϕ (this provides a resolution of about 6°), and the iteration process converged after 573 steps. Although there are some outlying points, the calculated surface energies are close to the model function. While the true depth of the cusp at (111) is not reproduced, the capillarity vector reconstruction method performs better than the series fitting method. Note that the only point where the discrete reconstructed data deviates significantly from the model function is at the (111) orientation. On later inspection, it was found that the randomly generated data set contained no grooves with these surfaces. While denser and more uniform trial data sets can be used to generate better reconstructions, the results shown in Fig. 2 are characteristic of the experimental data at hand and illustrate the challenges associated with discerning sharp features in the surface energy. 97% of the surface energies determined using the capillarity vector reconstruction method deviated from the model function by less than 0.04. In our reconstruction of the experimental data, we shall use this figure as a measure of the uncertainty in the result.

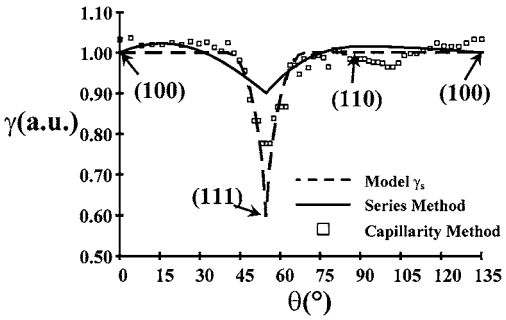

Figure 2. Plot of relative surface energies reconstructed from model data using both the series fit and capillarity vector reconstruction methods. The plot shows orientations around the perimeter of the unit triangle, from (100) to (111), then to (110), and back to (100).

(ii) Experimental Results

The reconstruction procedure was applied to the thermal groove measurements from a polycrystalline magnesia sample annealed in air at 1400°C. This is the same data set described in the previous paper and the results from the series fitting method are the same. As with the test data set, the sub-domain of surface characters was divided into 15 equal sections in $\cos(\theta)$ and ϕ; the iteration process converged after 27 steps. The values of the reconstructed surface energy at intervals around the perimeter of the unit triangle are shown in Fig. 3 and a contour plot illustrating the orientation dependence of the surface energy is shown in Fig. 4(a). Based on the capillarity vector reconstruction method,

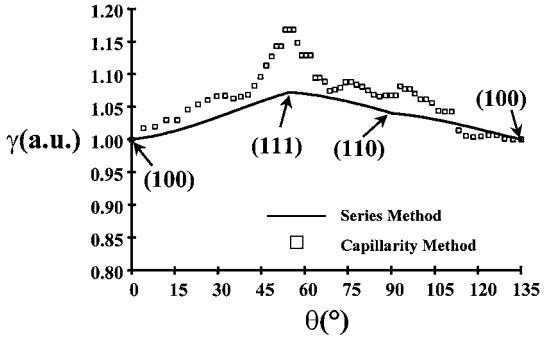

Figure 3. Comparison of the relative surface energies derived from the series fit and capillarity vector reconstruction methods for magnesia at 1400°C. The plot shows orientations around the perimeter of the unit triangle, from (100) to (111), then to (110), and back to (100).

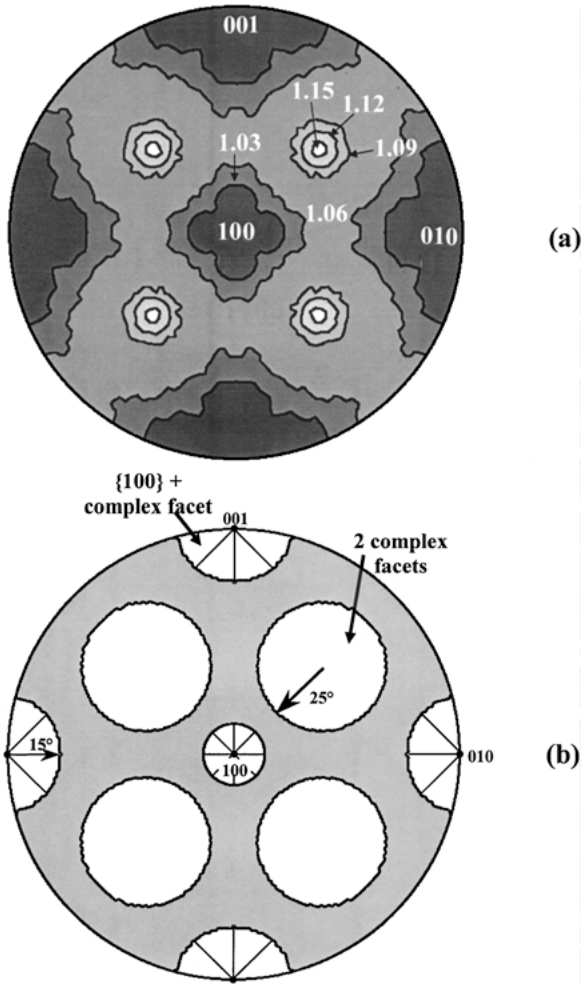

Figure 4. (a) Contour map on a stereographic projection of the relative surface energies derived from the capillarity vector reconstruction method for magnesia at 1400°C. (b) A schematic diagram summarizing observed orientation stability data for magnesia at 1400°C. Orientations near {100} are unstable with respect to faceting into the {100} orientation and a complex facet. The white regions around {111} correspond to unstable orientations which form two complex facets, while orientations in the shaded region are stable with respect to faceting.

the energies of the low index planes have the following relationships:

$$\frac{\gamma_{110}}{\gamma_{100}} = 1.07 \pm 0.04$$
$$\frac{\gamma_{111}}{\gamma_{100}} = 1.17 \pm 0.04$$

While the trends in the results from the series fitting method and the capillarity vector reconstruction method are the same, the later shows significantly more anisotropy. This is consistent with the results from model data sets. The reconstructed grain boundary energies are listed in Table 1.

Table 1. Reconstructed grain boundary energies.

γ_{gb}/γ_{100}	Misorientation,°
0.56	2.02
0.46	2.33
0.64	3.14
0.75	6.25
0.74	6.31

Discussion

The results from the capillarity vector reconstruction method suggest that the total anisotropy in the surface energy of magnesia is 17% while the results from the series fit method on the same data suggest an anisotropy of 7%. Based on the results from the reconstruction of the model data, we are led to believe that the capillarity vector reconstruction method produces more accurate results. Because the series fit results are constrained by the form of the basis functions, the full anisotropy can not be reproduced. The question is, which results more nearly represent the actual anisotropy? To discriminate between the two results, we can make a quantitative comparison between orientation stability data and the reconstructed surface energy.

In the previous paper, we examined the surfaces of 100 grains of known orientation by AFM and discriminated those that were faceted from those that were smooth [1]. The bounded and extended grain surfaces that have orientations that are part of the equilibrium crystal shape will remain flat during annealing. The surfaces of grains with missing orientations will form facets. Within about 15° of {100}, we find that surfaces facet to {100} plane and a complex facet. Further, all orientations within about 25° of {111} form two facets. These data are represented schematically in Fig. 4(b). At the time the previous paper was published, we were not able to unambiguously identify the facets formed on the surfaces near {111}. A careful examination of additional data has led us to the conclusion that both facets are always complex. In other words, the {111} surface, and those vicinal to it, are missing from the equilibrium shape. For any given orientation in this range, the facets and the macroscopic orientation must

share a common axis. This means that the missing orientation and the complex facets are in the same zone and lie on a great circle. Further, if the complex facets at the boundary of the unstable region have the same energy, then the circle should be the one that intersects the macroscopic orientation and has the minimum length through the unstable region. The orientation of the complex facets will be found at the intersection of this great circle and the boundary between the faceted and flat orientations.

The results from both the series fit method and the capillarity vector reconstruction method agree qualitatively with the observed faceting. To make a more quantitative comparison, we can assume that a local equilibrium is established at the intersections of the surface facets. Applying Herring's equation to this situation, we find that:

$$\frac{\gamma_1}{\gamma_2} = \cos\omega - \frac{1}{\gamma_2}\frac{\partial\gamma_2}{\partial\omega}\sin\omega \qquad (11)$$

where ω is the angle between the facets. An alternate expression, in terms of the capillarity vector, can be derived from Eq. (4). For simplicity, we will ignore to torque term and take the relative energy of two intersecting facets to be given by $\cos\omega$ (as long as one and only one is singular). If the (100) surface and the neighboring complex facets (with energy γ_c) are separated by 15°, then $\gamma_c/\gamma_{100} = 1.035$. Further, since the (111) facet is replaced by complex facets inclined by 25°, we conclude that γ_{111}/γ_c is 1.103. If we assume isotropy in this region of stable orientations, then the anisotropy we should expect between γ_{100} and γ_{111} to be the product of these two quantities, or about 14%. This is approximately double the amount of anisotropy predicted by the series fit method, which, in fact, predicted missing orientations only 4° from (100) and 5.5° from (111). The observed range of faceting more closely matches the results from the capillarity vector reconstruction method.

It is interesting to consider the reconstructed surface energies for missing orientations. When one examines the details of our measurement technique, it is clear that the energies of missing orientations should simply be the geometric combination of the energies of the stable facets that make up such orientations. While surfaces with missing orientations do not exist at any thermal groove root, faceted groove surfaces will have an effective or mesoscopic orientation in the missing range. This is the orientation that we observe. In earlier work, we described some of the difficulties associated with making accurate measurements of the surface inclination at the groove root [11]. Our conclusion was that the best measurements were made on relatively large grooves (greater than 2 μm wide). The width and depth of the groove are measured and then, assuming the known quasistatic profile, the inclination at the root is calculated [12, 13]. Because the surfaces we observed were faceted only on the nm-scale, thermal groove profiles on the micron scale remain smooth and "missing" orientations can be assigned to surfaces at groove roots that are actually faceted. In such cases, we assume that the mesoscopic shape of the groove is determined not by the particular facet that forms at the groove root 1 or 2 nm from the triple junction, but by the combination of the many small facets over which material must diffuse as the groove profile is established. This mesoscopic view of the groove is what determines the anisotropy in the range of missing orientations and the quantitative results reflect this approximation. For example, if the (111) surface were simply replaced by complex facets inclined at 25° (as observed), the increase in the surface energy based on the increase in surface area would be approximately 10%. In this same range of orientations, the results from the capillarity vector reconstruction method show an energy anisotropy of 9%. Finally, we should note that our mesoscopic approximation of the groove structure clearly breaks down when the size of the facets approaches the size of the groove.

Conclusion

When used to determine surface energy anisotropies from observations of grain boundary thermal grooves, the capillarity vector reconstruction method performs better than the series fit method. The capillarity vector reconstruction method does not assume a particular functional form for the surface energy and more accurately reproduces anisotropies. For MgO annealed at 1400°C in air, we find that the relative surface energies of the low index planes are $\gamma_{110}/\gamma_{100} = 1.07 \pm 0.04$ and $\gamma_{111}/\gamma_{100} = 1.17 \pm 0.04$.

Acknowledgments

This work was supported primarily by the MRSEC program of the National Science Foundation under Award Number DMR-0079996. The authors thank

A. Morawiec for useful suggestions and for communicating the results of his work prior to publication.

References

1. D.M. Saylor, D.E. Mason, and G.S. Rohrer, J. Am. Ceram. Soc. **83**, 1226 (2000).
2. W.A.Winterbottom and N.A. Gjostein, Acta Met. **14**, 1033 (1966).
3. M. McLean and B. Gale, Philos. Mag. **20**, 1033 (1969).
4. C. Herring, in *The Physics of Powder Metallurgy*, edited by W.E. Kingston (McGraw-Hill, New York, 1951), p. 143.
5. B. Gale, R.A. Hunt, and M. McLean, Philos. Mag. **25**, 947 (1972).
6. A. Morawiec, Acta Mater. **48**, 3525 (2000).
7. D.W. Hoffman and J.W. Cahn, Surface Science **31**, 368 (1972).
8. J.W. Cahn and D.W. Hoffman, Acta Met. **22**, 1205 (1974).
9. H.-J. Bunge, *Texture Analysis in Materials Science*, translated by P.R. Morris (Butterworths, London, 1982).
10. W.H. Press, B.P. Flannery, S.A. Teukolsky, and W.T. Vetterling, *Nurmerical Recipes in Pascal* (Cambridge University Press, Cambridge, 1989), p. 328.
11. D.M. Saylor and G.S. Rohrer, J. Am. Ceram. Soc. **82**, 1529 (1999).
12. W.W. Mullins, J. Appl. Phys. **28**, 333 (1957).
13. W.M. Robertson, J. Appl. Phys. **42**, 463 (1971).